

Virtual Reconstruction of broken and unbroken Pottery*

Martin Kampel and Robert Sablatnig

Vienna University of Technology

Institute for Computer Aided Automation

Pattern Recognition and Image Processing Group

Favoritenstrasse 9/183-2, A-1040 Vienna

kampel, sab@prip.tuwien.ac.at

Abstract

Motivated by the requirements of the present archaeology, we are developing an automated system for archaeological classification and reconstruction of ceramics. Due to the nature of ceramics, most of the excavated vessels are in the form of fragments called sherds. Only a few of the finds are complete, however these finds are the most important and interesting ones. Therefore we are developing a system that handles both complete and broken vessels using two different reconstruction strategies: A shape from silhouette based method for complete vessels and a profile based method for fragments. The profile is the cross-section of the fragment in the direction of the rotational axis of symmetry and can be represented by a closed curve in the plane. For complete vessels the 3D reconstruction is based on a sequence of images of the object taken from different viewpoints. Then the output of both algorithms is used to construct the 3D model of the vessel for classification and display.

1. Introduction

Ceramics are among of the most widespread archaeological finds, having a short period of use. Since the 19th century the physical characteristics of archaeological pottery have been used to assess cultural groups, population movements, inter-regional contacts, production contexts, and technical or functional constraints (archaeometry) [16]. Because archaeometry of pottery still suffers from a lack of methodology, it is important to develop analytical classification tools for artifacts [16]. A large number of ceramic fragments, called sherds, are found at every excavation. These fragments are documented by being photographed,

measured, and drawn; then they are classified. The purpose of *classification* is to get a systematic view on the excavated finds. Archaeological finds are traditionally grouped by typology. Defined forms and types of vessels form codes which simplify communication within the scientific field. The drawing in Figure 1 for instance is a representative of many other examples.

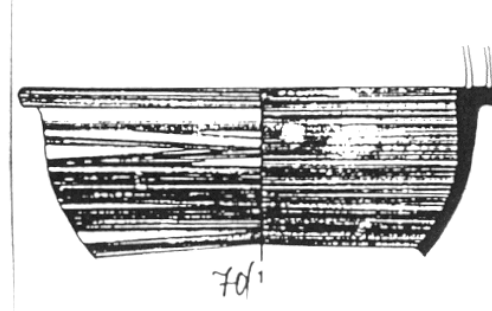


Figure 1. Drawing of a complete pot ([10])

The drawing and interpretation of ceramic fragments is very time consuming and costly, requiring trained and qualified draftsmen. The result is of course a simple 2D projection of the 3D object, therefore photographs of the real object must be added too. Nevertheless, there is no 3rd dimension left in the archive drawing and a graphic documentation done by hand also increases the possibility of errors. There may be errors in the measuring process (diameter or height may be inaccurate), and inconsistencies in the drawing of the fragment or the complete vessel. However it is not possible to achieve a consistent style, since it is very difficult to make a drawing of an object without interpretation. This leads to a lack of objectivity in the documentation of the material.

At excavations most of the finds are in form of fragments, only a few are still complete. It would be ideal to have one acquisition system that covers both sorts of objects, however, they do have different properties like dimen-

* This work was partly supported by the Austrian Science Foundation (FWF) under grant P13385-INF, the European Union under grant IST-1999-20273 , the Austrian Federal Ministry of Education, Science and Culture and by the innovative project '3D technology' of the Vienna University of Technology.

sions, color, and geometry. Fragments of vessels are thin objects, therefore 3D data of the edges of fragments are not accurate and this data can not be acquired without placing and fixing the fragment manually which is time consuming and therefore not practicable. Ideally, the fragment is placed in the measurement area, a range image is computed, the fragment is turned and again a range image is computed which leads us to the profile reconstruction method. Complete vessels, usually made on a rotation plate (potters wheel) can be recorded on a rotation plate too and therefore we choose this method.

Because the conventional documentation methods were shown to be unsatisfactory [16], the interest in finding an automatic solution increased. Existing techniques for solving the fragment reconstruction problem mainly focus on the analysis of the break curve [17]. In particular, Copper et. al. [3] developed a method for fragment matching based on a Bayesian approach using break curves, estimated axis and profile curves. Kong et. al. [12] try to solve the jigsaw problem in two stages: first, potsherds are joined automatically in two dimensions by using an efficient joint detection algorithm. Next, three dimensional shape is recovered by an adequate three dimensional transformation. Leitao and Stolfi [15] describe an algorithm for reassembling broken two-dimensional fragments. The procedure compares the curvature-encoded fragment outlines.

Figure 2 shows the inner side of a fragment on the left, its left side (broken surface) in the middle, and the profile section generated automatically on the right (Figure 1 shows the same fragment drawn by hand). We follow the profile approach as used by archaeologists for their reconstruction to reconstruct complete vessels out of fragments.



Figure 2. (a) Archaeological fragment - (b) site of fracture and - (c) profile section

For complete objects we use a combination of the *Shape from Silhouette* (SfS) method with the *Shape from structured Light* (SfL) method presented in [23]. The SfS approach is a method of automatic construction of a 3D model of an object based on a sequence of images of the object taken from multiple views, in which the object's silhouette represents the only interesting feature in the image [24, 18]. The object's silhouette in each input image corresponds to a conic volume in the object real-world space.

A 3D model of the object can be built by intersecting the conic volumes from all views, which is also called *Space Carving* [13]. The method can be applied on objects of arbitrary shapes, including objects with certain concavities, as long as the concavities are visible from at least one input view [25, 14]. This condition is hard to meet since most of the archaeological vessels have concavities that have to be modeled. Therefore, a second, active shape determination method (e.g. SfL) must be used to discover all concavities.

The paper is organized as follows: First we take a closer look on the acquisition devices used in order to get the 3D data of fragments and complete vessels in Section 2. Then we describe the reconstruction techniques used for fragments (Section 3) and complete vessels (Section 4) respectively. Reconstruction and visualisation results are given in Section 5, followed by conclusions and outlook on future work.

2. Acquisition System

The acquisition system consists of the following devices:

- the “Eyetronics Shape snatcher”: a Sony TVR-900E digital camera equiped with a Leica slide projector. Since it is a handheld device it is used for 3D recording of fragments on site.
- a turntable (Figure 3a) with a diameter of 50 cm, and a positional accuracy of 0.05°.
- two monochrome CCD-cameras with a focal length of 16 mm and a resolution of 768x576 pixels. One camera (*Camera-1* in Figure 3) is used for acquiring the images of the object's silhouettes and the other (*Camera-2* in Figure 3) for the acquisition of the images of the laser light projected onto the object.
- a red laser (Figure 3d) used to project a light plane onto the object. The laser is equipped with a prism in order to span a plane out of the laser beam.
- a lamp (Figure 3e) used to back-light [8] the scene for the acquisition of the silhouette of the object.

The acquisition method for estimating the 3D-shape of a fragment is shape from structured light [5], which is based on active triangulation [1]. We used the *Eyetronics Shape Snatcher Technology* [6], that allows to generate 3D models based on the use of a single image taken by an ordinary camera. The image obtained is a 2D array of depth values called a range image.

The geometrical setup of the acquisition devices used for complete vessels is shown in Figure 3. Both b/w cameras are placed about 50 cm away from the rotational axis of the turntable. Ideally the optical axis of the camera for acquiring object's silhouettes lies nearly in the rotational plane of

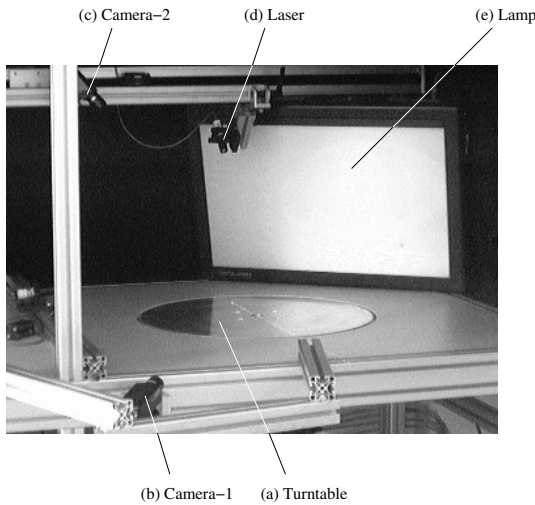


Figure 3. Acquisition System

the turntable, orthogonal to the rotational axis. The camera for acquiring the projection of the laser plane onto the object views the turntable from an angle of about 45° . The laser is directed such that the light plane projected contains the rotational axis of the turntable. Prior to any acquisition, the system is calibrated in order to determine the inner and outer orientation of the cameras and the rotational axis of the turntable (for details see [25]). The whole system is protected against the ambient light by a thick black curtain.

3. Fragment Reconstruction from Profiles

Archaeological pottery is assumed to be rotational symmetric since it was produced on a rotation plate. With respect to this property the axis of rotation is calculated using a Hough inspired method [22]. To perform the registration of the two surfaces of one fragment, we use a-priori information about fragments belonging to a complete vessel: both surfaces have the same axis of rotation since they belong to the same object. If one wants to reconstruct the complete vessel out of the fragment, orientation and diameter (which is in fact the exact computation of the axis of rotation in 3D) are of central concern. We concentrate on the registration of the front- and back-view of one fragment which is significantly different from registering the surfaces of different fragments of one object in order to reconstruct the object out of its pieces.

Pottmann et al. [19] proposed a solution to reconstruct helical surfaces or surfaces of revolution using line geometric concepts. Their algorithm is based on the fact that the normals of the surfaces lie in linear complices. Our estimation of the axes of rotation exploits the fact that surface normals of rotationally symmetric objects intersect their axis of

rotation. The basis for this axis estimation is a dense range image provided by the range sensor. If we have an object of revolution, like an archaeological vessel made on a rotation plate, we can suppose that all intersections n_i of the surface normals are positioned along the axis of symmetry a .

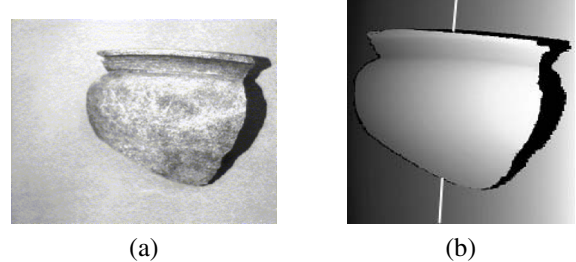


Figure 4. Intensity image (left) and range image (right) of a fragment with rotational axis of the front-view.

Figure 4a shows the intensity image for a front-view of a fragment, Figure 4b shows the result on the range image with the estimated rotational axis. (black regions in Figure 4b indicate points where no range information is available due to occlusion of light stripes).

To perform the registration of the two surfaces, we use a-priori information about fragments belonging to a complete vessel: both surfaces have the same axis of rotation since they belong to the same object. Furthermore, the distance of the inner surface to the axis of rotation is smaller than the distance of the outer surface. Finally, both surfaces should have approximately the same profile; i.e. the thickness of the fragment measured on a plane perpendicular to the rotational axis should be constant in the average.

The goal of the registration is to find the transformation that relates these two views to one another, thus bringing them into alignment so that the two surfaces represent the object in 3D [2]. The most commonly used algorithm for registering is the ICP algorithm [7]. ICP iteratively improves the registration of two overlapping surfaces by calculating the unique transformation that minimizes the mean square distances of the correspondences between the two surfaces. The algorithm starts with the selection of some point sets in one or both surfaces (which generally are triangulated surfaces), matches these point sets to one another, which gives a set of corresponding pairs and weights the corresponding pairs. A rejection rule for pairs is applied to all pairs to determine outliers. To measure the fit, an error metric is used, which is minimized iteratively. There are many different variants of the ICP Algorithm (see [21] for a review) all based on local point correspondences. Therefore, it is very important to have a good rough alignment of the surfaces to be registered.

We register the range images by calculating the axis of

rotation of each view and by bringing the resulting axes into alignment. Knowing the surface normals of all surface patches we transform them into a common reference coordinate system. The first rough alignment is performed by aligning the two surfaces vertically. Next we perform the horizontal alignment by rotating one surface relative to the other until both surfaces have a maximum number of points in a common projection normal to the fixed surface.

In the next step we have to align the surfaces of the objects to avoid intersecting surfaces. The correct match is calculated using a slightly modified ICP algorithm [20]. The difference to the standard ICP is that we are calculating the unique transformation that minimizes the mean square distances of the correspondences between the two surfaces to a constant value instead to zero. This distance is the distance of the two surfaces on a plane perpendicular to the rotational axis. A detailed description of the registration algorithm can be found in [22].

Figure 5 shows the registration of intersecting surfaces for real data in detail: Figure 5a and Figure 5b show intersecting surfaces due to incorrect rotational axis estimation, Figure 5c shows the same surfaces after the ICP-based registration procedure.

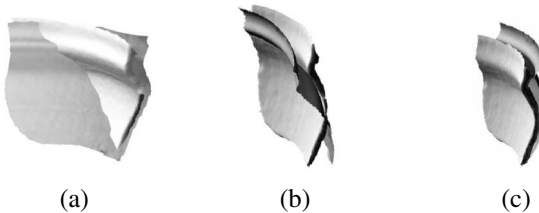


Figure 5. Registration steps using real data.

Figure 6 shows the 3D-model of a sherd and its rotational axis rot as a vertical line along the z-axis. The black plane represents the intersecting plane e_{max} at the maximum height h_{max} of the sherd. The longest profile line is supposed to be the longest elongation along the surface of the sherd parallel to the rotational axis rot . The extracted profile line is shown in the xz-plane. Our algorithm for the estimation of the longest profile line consists out of the following steps:

1. First the axis of rotation is transformed into the z-axis of the coordinate system in order to simplify further computation.
2. The fragment's size is described by its circular arc. Depending on the size we compute a number of intersecting planes e_i , which are used for the profile estimation. The number of planes e_i depends on the length of the perimeter of the fragment. Experiments have shown that 7 to 13 profile lines return the best ratio of exactness and performance.

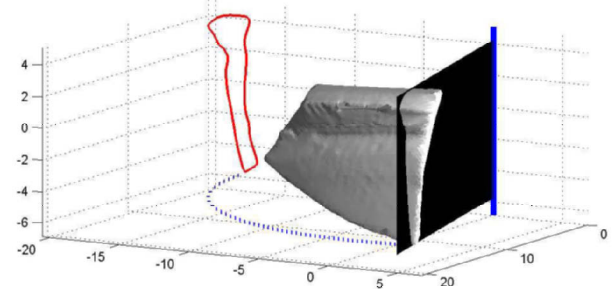


Figure 6. Orientated sherd, rotational axis, intersecting plane e_{max} , longest profile line

3. A profile line is calculated by intersecting the 3D-data of the fragment with planes e_i : First the distance of each vertex of the fragment to the plane e_i is calculated. All vertices are sorted by their distance to the plane. Then the nearest 1% of vertex are selected as candidates for the profile. For each of those vertices all the patches they belong to are filtered through a search in the patch list with their index number. Every patch is a triangle which consists of three points that are connected through three lines. Every pair of vertices that have a point on each side of the plane is part of the profile line, because its connection intersects the plane. The coordinates of these pairs are rotated into the xy-plane and the z-coordinate is removed. The result is a properly oriented profile line.
4. Next the profile line with the longest elongation is computed: the difference between the maximum z-value and the minimum z-value of the profile line defines the height of the profile line. The remaining profile lines are used for evaluation of the estimation of the rotational axis.

The registration of front- and back-view together with the axis of rotation provide the profile used to reconstruct the vessel. This reconstruction is only complete in the sense that the profile is rotated around the axis of rotation and thus constructs a 3D object. If one wants to really reconstruct one complete vessel out of one (possibly small) fragment a classification of the fragment has to be performed first which then gives a number of similar fragments of which the complete profile can be estimated and manually selected by an expert (see [9] for details).

4. Reconstruction of Complete Vessels

An input image for Shape from Silhouette defines a conic volume in space which contains the object to be modeled (Figure 7a). Another input image taken from a different

view defines another conic volume containing the object (Figure 7b). Intersection of the two conic volumes narrows down the space the object can possibly occupy (Figure 7c). With an increasing number of views the intersection of all conic volumes approximates the actual volume occupied by the object better and better, converging to the 3D convex hull of the object. Therefore by its nature Shape from Silhouette defines a *volumetric* model of an object.

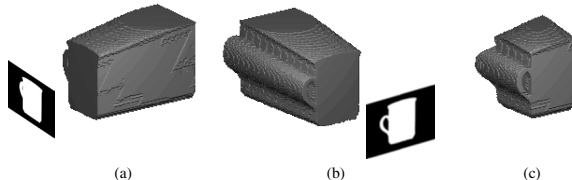


Figure 7. Two conic volumes and their intersection

An input image for SfL using laser light defines solely the points on the surface of the object which intersect the laser plane. Multiple views provide a cloud of points belonging to the object surface, which is a *surface* model of the object.

Our approach builds a 3d model of an object performing the following steps (illustrated in Figure 8): First, both of the input images (SfS and SfL) are binarized such that the white image pixels *possibly* belong to the object and the black pixels *for sure* belong to the background (Figure 8a). Then, the initial octree containing one single root node marked "black" is built (Figure 8b). Black nodes are subsequently checked by projecting the nodes into all SfS binarized input images and intersecting them with the image silhouettes of the object (Figure 8c). As the result of the intersection the node can remain "black" (if it lies within the object) or set to "white" (it lies outside the object) or "grey" (it lies partly within and partly outside the object). If the resulting node is not white, it is projected into the binarized SfL image representing the nearest laser plane to the node and again intersected. All grey nodes are divided into 8 child nodes all of which are marked "black" and the intersection test is performed in each of the black nodes. This subdivision of grey nodes is done until there are no grey nodes left or a subdivision is not possible (voxel size), which results in the final model (Figure 8d). A detailed description of the algorithm can be found in [23].

5. Results

The resulting 3D reconstruction of fragments depends on the correct orientation of the profile section. The evaluation of the 3D representation is rather complicated since ground truth is not available due to the fact that there is no 3rd di-

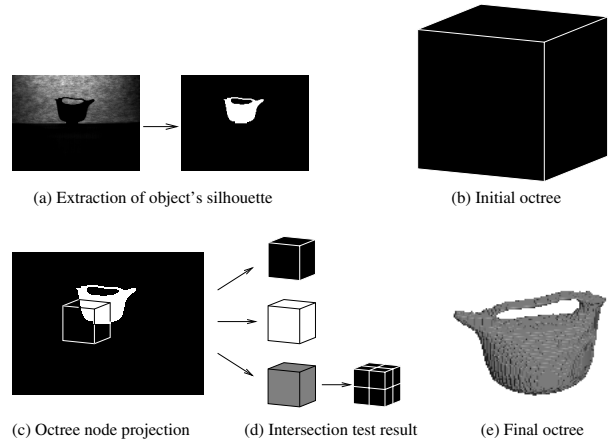


Figure 8. Algorithm overview

mension in archaeological archive drawings and the object does not exist in reality. The description of shape is subject to the ideas of the authors and is not standardized. Experiments on synthetic fragments, cheap flowerpots intentionally broken and archaeological fragments are described in detail in [22].

In order to demonstrate the correctness of the computed profile lines Figure 9 shows a recorded sherd (dark object) and its computed profile section (vertical line). The computation of the virtual fragment (grey object) is based on the profile section. One can see that the recorded fragment fits into the virtual fragment, which indicates that the computation is correct. Following multiple cross-sections along the perimeter of the virtual fragment - Figure 10 - one can observe hardly any deviation from the original fragment. Some are caused by the bumpiness of the surface, because the surface is not exactly rotationally symmetric, since it is hand-made pottery.

If the fragment was orientated incorrectly as shown in Figure 11, the recorded fragment does not fit into the virtual object and multiple cross-sections along the perimeter of the virtual fragment show large deviations from the original object (see Figure 12). The success rate for correct extraction of the profile line and consequently the percentage of sherds which is used for further classification is around 50% of the data found at the excavation site. This has to be seen with respect to manual archivation done by archaeologists [16]: for coarse ware around 35% [4] and for fine ware around 50% [4] of the findings are used for further classification. It depends heavily on the shape of the fragment (e.g. handle, flat fragments like bottom pieces, small size, etc.).

As a result the profile was constructed from methods described in Section 3. A profile computed was rotated 360 degrees around the axis of rotation in order to construct the vessel in 3D. Next the resulting 3D point cloud was triangulated [11] and the acquired texture was mapped onto the

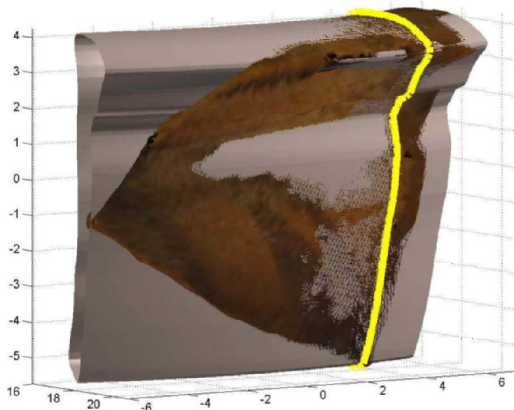


Figure 9. Reconstructed fragment, profile section and recorded fragment

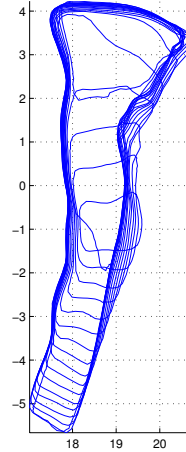


Figure 10. Cross- sections of the original fragment along the perimeter of the virtual fragment

triangulated mesh. Figure 13 shows the reconstructed pot.

The reconstruction of complete vessels was tested on synthetic and real objects: For tests with synthetic objects we can build a model of a virtual camera and create input images such that the images fit perfectly into the camera model. In a test we built models using 360 views with a constant angle of 1° between two views, while increasing octree resolution. It turned out that the shape from Silhouette method performed best with an octree resolution of 128^3 , where the approximation error was $+0.83\%$ of the actual volume.

For tests with real objects we use 5 objects: a metal cuboid, a wooden cone, a coffee mug, and two archaeological vessels. The cuboid and the cone have known dimensions so we can calculate their volumes analytically and compare them with the volumes of their reconstructed models. Using these two objects we can also measure the impact of ignoring camera lens distortion on the accuracy of the models: The models built taking lens distortion into account were always slightly better ($0.5\% - 1.5\%$) than the models built ignoring it, but there was no significant difference, which can be expected when the objects stay mainly close to the center in all input images. Ignoring camera lens distortion reduces the time needed to build a model by 75%.

All models shown in this section are built using 360 views, with constant angle of 1° between two neighboring views. Table 1 summarizes the results. The resulting models, shown from three views, are depicted in Figure 14. All models are built with an octree resolution of 256^3 and using 360 views.

<i>object</i>	<i>voxel size</i>	<i>measured dimensions (mm)</i>
cuboid	0.50 mm	$100 \times 70 \times 60$
cone	2.00 mm	$156 \times 156 \times 78$
vessel #1	0.74 mm	$141.2 \times 84.8 \times 93.7$
vessel #2	0.53 mm	$114.2 \times 114.6 \times 87.4$
cup	0.66 mm	$X \times X \times X$
<i>object</i>	<i>volume(mm^3)</i>	<i>measured dimensions (mm)</i>
cuboid	$384\,678 (-8.41\%)$	$101 \times 71 \times 60$
cone	$435\,180 (-12.43\%)$	$150.1 \times 149.4 \times 77.5$
vessel #1	$336\,131$	$139.2 \times 83.2 \times 91.4$
vessel #2	$263\,696$	$113.0 \times 111.9 \times 86.4$
cup	$276\,440$	$111.6 \times 79.0 \times 98.3$

Table 1. Reconstruction of cuboid, cone, two vessels, and a cup

6. Conclusion and Outlook

In this paper a Shape from Structured Light method to reconstruct a vessel out of a fragment and a Shape from Silhouette method to reconstruct complete archaeological vessels were presented. For fragments, the profile, which is the cross-section of the fragment in the direction of the rotational axis of symmetry, represented by a closed curve in 2D, is computed by registering the front- and the back-view of the fragment to one another. Within the registration process, the axis of rotation is computed which is then used to reconstruct the complete shape. For complete vessels the 3D model of an object is constructed from images of the object taken from different viewpoints. The algorithm employs only simple matrix operations for all the transformations and it is fast, because even for highly detailed objects, a high resolution octree (256^3 voxels) and a high number of input views (36), the computational time hardly exceeded

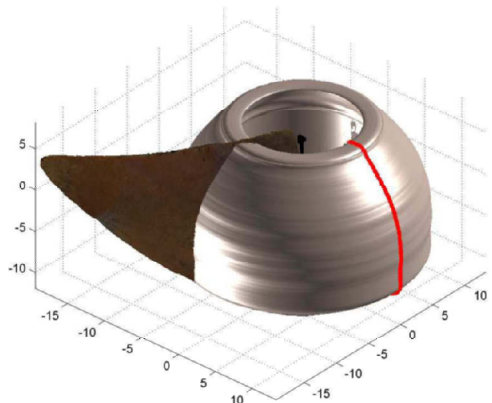


Figure 11. Incorrect reconstruction of a fragment due to incorrect orientation

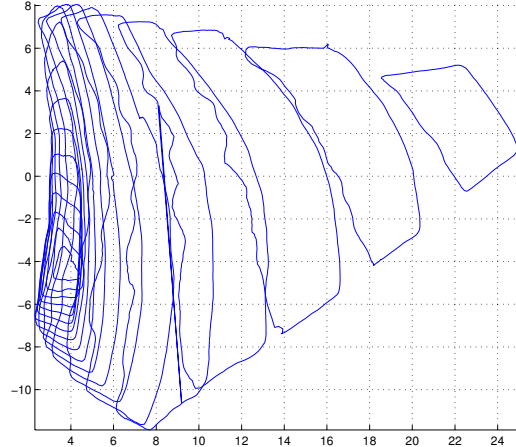


Figure 12. Cross- sections of the original fragment along the perimeter of the virtual fragment

1 minute on a Pentium II. Already for a smaller number of views (12) the constructed models were very similar to the ones constructed from 36 views and they took less than 25 seconds of computational time.

For archaeological applications, the object surface has to be smoothed in order to be applicable to texture mapping and therefore ceramic documentation. For classification, however, the accuracy of the method presented is sufficient since the projection of the decoration can be calculated and the volume estimation is much more precise than the estimated volume performed by archaeologists.

The ceramic documentation and reconstruction system described is currently under further development to be integrated in the virtual excavation reconstruction project 3D MURALE [6]. Currently we are working on the classification system based on the profile in order to classify all profiles and to find matching fragments from similar vessels and finally the same vessel.

References

- [1] P.J. Besl. Active, Optical Range Imaging Sensors. *MVA*, 1(2):127–152, 1988.
- [2] B. Bhanu. Representation and Shape Matching of 3D Objects. *IEEE Trans. on Pattern Analysis and Machine Intelligence*, 6(3), 1984.
- [3] D. Copper and et al. Bayesian pot-assembly from fragments as problems in perceptual-grouping and geometric-learning. In R. Kasturi, D. Laurendeau, and C. Suen, editors, *Proc. of 16th International Conference on Pattern Recognition*, Quebec City, volume 1, pages 297–302. IEEE Computer Society, 2002.
- [4] R. Degeest. The Common Wares of Sagalassos. In M. Walken, editor, *Studies in Eastern Mediterranean Archaeology*, III, 2000.
- [5] F. DePiero and M. Trivedi. *3D Computer Vision using Structured Light: Design, Calibration, and Implementation Issues*. Advances in Computers, 1996.
- [6] J. Cosmas et al. 3D MURALE: A Multimedia System for Archaeology. In *Proc. of Intl. EuroConference on Virtual Reality, Archaeology and Cultural Heritage*, Athens, Greece, 2001.
- [7] M. Greenspan and Godin G. A Nearest Neighbor Method for Efficient ICP. In *Proc. of the 3rd IEEE*

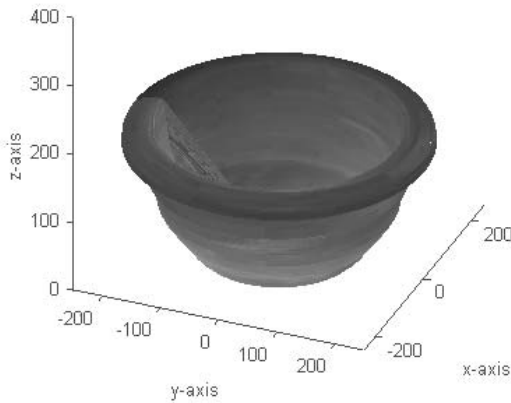


Figure 13. 3D reconstruction out of a profile section

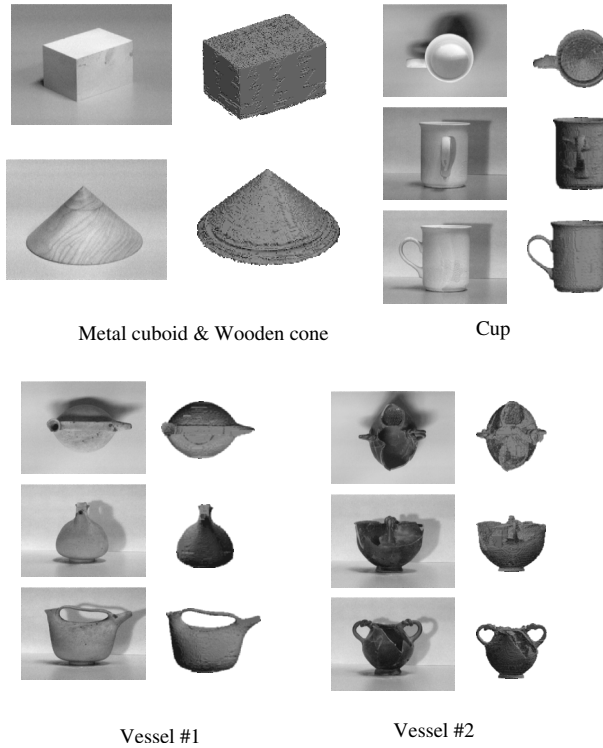


Figure 14. 3D models of cuboid, cone, two vessels, and a cup

Intl. Conference on 3-D Digital Imaging and Modeling, Quebec, pages 161–168, 2001.

- [8] R. M. Haralick and L. G. Shapiro. Glossary of computer vision terms. *PR*, 24(1):69–93, 1991.
- [9] M. Kampel, R. Sablatnig, and E. Costa. Classification of Archaeological Fragments using Profile Primitives. In S. Scherer, editor, *Proc. of 25th AAPR Workshop*, pages 151–158, 2001.
- [10] P.M. Kenrick. *Rim-forms of some Relief-decorated Vessels in Italian Terra Sigillata*. Conspectus formarum terrae sigillatae italico modo confectae. Bonn, 1990.
- [11] R. Klette, A. Rosenfeld, and F. Sloboda. *Advances in Digital and Computational Geometry*. Springer Singapore, 1998.
- [12] W. Kong and B.B. Kimia. On solving 2d and 3d puzzles using curve matching. In *IEEE Computer Society Conference on Computer Vision and Pattern Recognition (CVPR '01)*, volume 2, pages 583–590, 2001.

- [13] K.N. Kutulakos and S.M. Seitz. A Theory of Shape by Space Carving. *International Journal of Computer Vision*, 38(3):197–216, July 2000.
- [14] A. Laurentini. How Far 3D Shapes can be Understood from 3D Silhouettes? *IEEE Transactions on Pattern Analysis and Machine Intelligence*, 17(2), 1995.
- [15] H. C. G. Leitao and J. Stolfi. A Multiscale Method for the Reassembly of Two-Dimensional Fragmented Objects. *IEEE Trans. on Pattern Analysis and Machine Intelligence*, 24(9), 2002.
- [16] C. Orton, P. Tyers, and A. Vince. *Pottery in Archaeology*. Cambridge University Press, 1993.
- [17] G. Papaioannou, E.A. Karabassi, and T. Theoharis. Virtual archaeologist: Assembling the past. *IEEE Computer Graphics*, 21(2):53–59, March-April 2001.
- [18] M. Potmesil. Generating Octree Models of 3D Objects from Their Silhouettes in a Sequence of Images. *CVGIP*, 40:1–29, 1987.
- [19] H. Pottmann, M. Peternell, and B. Ravani. An Introduction to Line Geometry with Applications. *Computer-Aided Design*, 31:3–13, 1999.
- [20] K. Pulli. Multiview Registration for Large Data Sets. In *Proc. of the 2nd IEEE Intl. Conference on 3-D Digital Imaging and Modeling, Ottawa*, pages 160–168, 1999.
- [21] S. Rusinkiewicz and Levoy M. Efficient Variants of the ICP Algorithm. In *Proc. of the 3rd IEEE Intl. Conference on 3-D Digital Imaging and Modeling, Quebec*, pages 145–152, 2001.
- [22] R. Sablatnig and M. Kampel. Model-based Registration of Front- and Backviews. *Computer Vision and Image Understanding*, 87(1):90–103, 2002.
- [23] Robert Sablatnig, Srdan Tosovic, and Martin Kampel. Combining Shape from Silhouette and Shape from Structured Light for Volume Estimation of Archaeological Vessels. In R. Kasturi, D. Laurendeau, and C. Suen, editors, *Proc. of 16th International Conference on Pattern Recognition, Quebec City*, volume 1, pages 364–367. IEEE Computer Society, 2002.
- [24] R. Szeliski. Rapid Octree Construction from Image Sequences. *CVGIP: Image Understanding*, 58(1):23–32, 1993.
- [25] S. Tosovic and R. Sablatnig. 3d Modeling of Archaeological Vessels using Shape from Silhouette. In *Proc. of 3rd IEEE Intl. Conference on 3-D Digital Imaging and Modeling, Quebec, Canada*, pages 51–58, 2001.